

## Size distribution of marine submicron particles determined by flow field-flow fractionation

**Abstract**—Flow field-flow fractionation (flow FFF) with power field-strength programming was used to size fractionate submicron particles (colloids) in coastal seawater. All analyses used filtered seawater as carrier solution to preserve the native chemical environment of the colloids. Our fractograms show colloid size distributions with major peaks centered at 50 to 60 nm for samples that were size fractionated immediately following the preconcentration step. Preconcentrated samples that had aged for 2 to 5 d revealed the presence of an additional larger sized particle (or aggregate) peak with indeterminate size. Errors in colloid sizing may result if the physical and chemical behaviors of the particle size standards are not mimicked by those of the colloids during separation in the flow FFF channel. Particle detection using absorbance meters, such as the ultraviolet (UV) detector used here, greatly underestimates the contribution of smaller particles (ca. <100 nm) due to the exceedingly small optical efficiency of particles within this size-refractive index domain.

Colloids in aquatic environments have been defined as that fraction of the pool of matter whose equivalent spherical diameter falls within the size range of 1 to 1,000 nm (Vold and Vold 1966). The colloidal state contains such diverse matter as viruses, aggregated organic polymer gels, globular and fibrillar exopolymers of polysaccharides and proteins, fulvic and humic acids, and inorganic particles such as metal oxides, silica, and clay minerals. Some microorganisms also fall within this size range and may be included as colloidal, although their contribution to the total pool of colloidal organic matter may be very low (Koike et al. 1990). Colloids in aquatic environments have been implicated in biogeochemical cycling and transport of organic matter (Koike et al. 1990; Kepkay 1994; Wells and Goldberg 1994), fate and transport of heavy metals and pollutants (Honeyman and Santschi 1991), and light scattering (Stramski and Kiefer 1991).

There has been a diversity of methods used for sizing aquatic colloids, each with its inherent limitations and assumptions. Membrane ultrafiltration methods, although problematic (*see* review in Brownawell 1991), provided valuable data on the relative amounts of organic carbon within a few broadly defined size categories defined by the retention characteristics of the filter membranes used (Maurer 1976; Buffle et al. 1978; Zsolnay 1979). Resistive-pulse particle counting and laser-light scattering enabled size analysis of colloids in their native chemical environment with minimal sample manipulation, but were limited by detector sensitivity to enumeration of larger (ca. >0.4  $\mu\text{m}$ ) colloids only (Koike et al. 1990; Longhurst et al. 1992; Chin et al. 1998). Transmission electron microscopy (Harris 1977; Wells and Goldberg 1991, 1994; Santschi et al. 1998) and atomic force microscopy (Santschi et al. 1998) allowed the direct observation of colloids and sizing down to about 1 nm. However, the sample

preparation undoubtedly exposed the colloids to rapid changes in ionic strength and pH, which have been shown to alter the hydrodynamic diameter and shape of organic polymer gels (Chin et al. 1998).

Here we present preliminary data describing the efficacy of a flow FFF method for determining marine colloid size distributions. We present some data on particle size distributions from local marine harbor samples to demonstrate its applicability to marine waters and to suggest some improvements on the method. The advantage of this method over others is its ability to provide uniform fractionating power over a wide range of particle diameters (~4 to 1,000 nm) encompassing nearly the entire size range of particles typically defined as colloidal (Vold and Vold 1966). Also, the separation takes place in a seawater carrier solution, thus minimizing changes in colloid conformation and size related to changes in pH and ionic strength. The flow FFF technique has been used successfully by others to measure the size distribution and diffusion coefficients of various colloid-sized particles (Giddings et al. 1977) and humic substances from fresh water environments (Beckett et al. 1987).

**Theory and methods**—Flow field-flow fractionation is a chromatographic-like analytical method for the separation of particles and macromolecules based on their diffusion coefficients. The column is an unpacked thin ribbon channel whose flat sides are composed of porous frits bounded on one side by a semipermeable membrane. Filtered-seawater carrier solution is pumped by two precision pumps through the channel, independently and at right angles to one another. The flow down the long axis of the channel is laminar and has a parabolic profile with faster flow velocities in the center than nearer the edges. Orthogonal to this flow is the cross-flow stream, which passes out one porous frit through the semipermeable membrane and out the second frit. Sample is injected into one end of the column. The channel flow is interrupted for a brief period while the particles migrate to equilibrium positions across the thin axis of the channel such that particle diffusion is balanced by the cross-flow velocity. The channel flow resumes and the particles are carried along the long axis of the channel in the laminar flow. Retention time in the channel is determined by particle positions in the laminar flow field, with lower retention for particles positioned in the faster moving channel center and higher retention for those situated within the slower moving flow nearer the edges. The retention volume of the particle can be related precisely to the particle's diffusion coefficient through mathematical relationships describing particle behavior in a channel with well-defined dimensions and cross-flow velocity. The diffusion coefficient can then be related to particle diameter through the Stokes-Einstein equation. A

more mathematical treatment of flow FFF theory can be found in Giddings et al. (1976, 1977).

Size fractionation of particles and molecules using flow FFF utilizing a constant cross-flow rate is generally useful for separation of analytes with only minor (ca. <50-fold) differences in hydrodynamic diameters. Since the diameter range of colloids encompasses 3 orders of magnitude (1 to 1,000 nm), we employed power-programmed field decay. With power programming, the cross-flow velocity decays with time according to a power law, resulting in uniform fractionating power over a wider range of particle sizes than is achievable with a constant field strength (Williams and Giddings 1987).

The experimental setup consisted of a model F-1000 universal fractionator with frit outlet (FFFractionation, LLC). The channel was composed of two acrylic blocks with ceramic frits, between which was placed a 0.025 cm polyester spacer with a regenerated cellulose membrane of nominal molecular weight cutoff of 10,000 daltons (ca. 3-nm equivalent spherical diameter). An SSI series II pump (Scientific Systems) controlled the flow of carrier liquid down the long axis of the channel (channel flow), and a Pharmacia P-500 pump (Pharmacia Biotech AB) controlled the perpendicular flow (cross-flow). Teflon tubing connected all the components, and a Rheodyne model 7725 injector with a 100- $\mu$ l sample loop served to introduce the sample to the channel. A recirculated cross-flow stream was used to maintain a uniform cross-flow force field. Channel flow exited the channel at two points at the terminus of the channel block: at the outlet to the detector and, just upstream, at the frit outlet. A needle valve was placed at the terminus of the frit outlet tube to restrict flow here and redirect carrier, enriched with particles, to the detector outlet. Careful adjustment of the frit outlet needle valve resulted in sample enrichment and lowered detection limits by this technique. We used an ultraviolet (UV) absorbance detector (Alltech Model 450 UV at 254 nm, Alltech Associates) set at its highest sensitivity setting of 0.005 absorbance units for full-scale deflection. Carrier solution flowed through the detector reference loop to provide baseline stability. Software supplied with the instrument controlled the cross-flow pump rates and recorded the detector response digitally.

Seawater was sampled from the dock at Bigelow Laboratory for Ocean Sciences, West Boothbay Harbor, Maine, and was used for both sample and carrier solution. To the seawater carrier was added a biological nonionic surfactant (Pluronic® F68, BASF) to a final concentration of 0.1% (v/v) to help minimize ionic interactions between particles. The carrier solutions were vacuum filtered through 0.2- $\mu$ m polycarbonate membrane filters and then heated under vacuum to sparge dissolved gases. Carrier solutions prepared in this manner exhibited very low baseline noise at the highest sensitivity detector settings. Since the carrier is natural, filtered seawater, it also contains submicron particles less than 0.2- $\mu$ m diameter. These particles are present in concentrations far below those in the preconcentrated seawater sample and do not contribute to the measured mass signal because the carrier solution passes through the reference cell of the detector as well.

The sample was prepared by preconcentration of up to 2.5

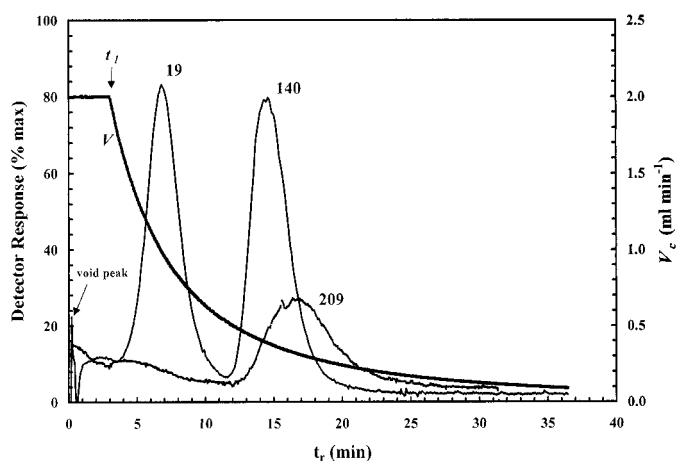


Fig. 1. Polystyrene latex beads separated using power-law cross-flow decay program. The cross-flow field  $V_c$  decayed as a function of time according to  $V_c(t) = V_0[t_1 - t_d/t - t_a]^p$  (Williams and Giddings 1987), where  $V_0$  the initial constant cross-flow rate = 1.94 ml min<sup>-1</sup> for  $t_1 = 3$  min, the channel flow rate  $V = 4.12$  ml min<sup>-1</sup>,  $t_a$  is a parameter controlling the rate of decay = -6 min, and the exponent  $p = 2$ . The  $V_c$  at the end of the decay program was 0.1 ml min<sup>-1</sup>. The carrier solution was seawater ( $S = 30\%$ ). The absorbance data were acquired every 4.5 s. Volume of the detector cell was 0.013 cm<sup>3</sup>, and the flow rate through the cell was 1 to 1.5 ml min<sup>-1</sup>. Thus, each data point represents the absorbance value for 0.008 to 0.0125 cm<sup>3</sup> of sample measured every 4.5 s.

liters of seawater through a 200-ml Amicon® stirred-cell concentrator (Millipore) at room temperature using an Amicon YM-10 membrane (nominal molecular weight cutoff of 10,000 daltons, or ca. 3 nm). Nitrogen gas pressure of 60 to 70 psi was used to push the liquid through the membrane. Preconcentration of smaller volume samples was done in Ultrafuge® centrifuge filters (Micron Separations) with polysulfone membranes of the same membrane pore-size as the Amicon cell. We used monodisperse suspensions of polystyrene (PS) latex beads (Coulter, Polysciences and Duke) ranging in diameter from 19 to 1,000 nm to develop a standard curve relating retention volume to particle diameter in the size range of marine colloids.

**Results and discussion**—A sample fractogram showing the size distributions for suspensions of three different size beads eluted with a power-programmed cross-flow field is shown in Fig. 1. The bead profiles were always well resolved from the void peak ( $R = V^0/V_r$  mean value = 0.02 ± 0.03 s.d.; range 0.007–0.11) and routinely exhibited sharp, Gaussian-shaped peaks with minimal skewness. A standard curve plot of  $V_r$  versus log<sub>10</sub> of bead diameter exhibited considerable scatter, but with a significant log-linear trend line with an  $r$  squared value of 0.77 (Fig. 2).

We compared the experimental retention volumes for each PS bead to its theoretical  $V_r$  (Williams and Giddings 1987) to determine to what extent the PS beads exhibited ideal retention behavior using power-programmed field-strength decay. Figure 3 shows the results of this comparison for 44 analyses using identical conditions of power-programmed field-strength decay and carrier solution. There was a large

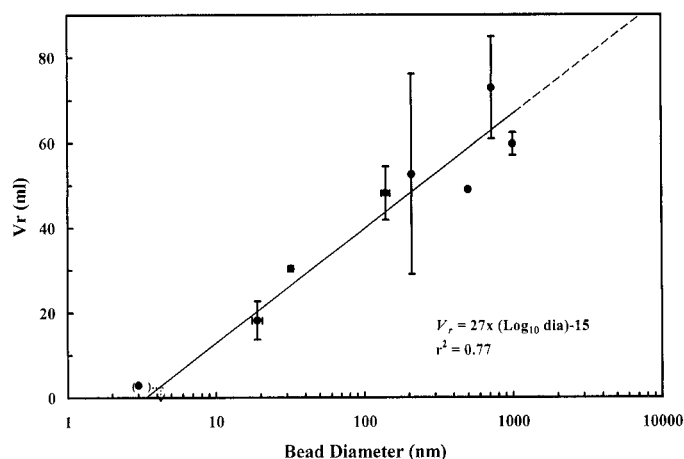


Fig. 2. Volume retention of polystyrene latex beads in seawater carrier solution. The carrier contained 0.1% pluronic F68 surfactant. Each symbol represents the mean value and the error bars  $\pm$  one standard deviation (s.d.). The mean bead diameters  $\pm$  s.d. were supplied by the bead manufacturers, and the retention times were the mean  $\pm$  s.d. values for  $n$  replicate analyses (19-nm beads,  $n = 22$ ; 32-nm beads,  $n = 1$ ; 140-nm beads,  $n = 9$ ; 209-nm beads,  $n = 4$ ; 501-nm beads,  $n = 1$ ; 723-nm beads,  $n = 2$ ; 1,000-nm beads,  $n = 2$ ). The symbol in parentheses in the lower left is bovine serum albumin (BSA) and is not included in the regression calculation.

amount of scatter in the data, but an overall trend was evident with a slope value less than the expected value of one. Beads smaller than approximately 500 nm generally exhibited retarded retention in the channel, while those larger than this size eluted sooner. We do not know the reasons for this anomalous behavior, but hypothesize that the polystyrene beads exhibited nonideal electrostatic attractive forces due to the natural surfactant present in the seawater carrier solution coating the channel surfaces (Neihof and Loeb 1972; Loeb and Neihof 1977). Thus, the observed log-linear relationship between bead diameter and retention time (Fig. 2) was not predictable solely by the diffusive properties of the beads.

The smallest diameter particle resolvable by this method can be estimated by calculating the particle diameter that eluted in the void peaks. The mean void peak retention volume ( $V_{r,0}$ ) for the 44 polystyrene bead runs was 0.8 ml ( $\pm$  s.d. = 0.5 ml), which is equivalent to a particle diameter of 3.9 nm, close to the regression line  $x$ -axis intercept of 3.6 nm. Bovine serum albumin (BSA), a globular protein (molecular weight 66,000 daltons), was included to test the method's ability to correctly size a large nonspherical water-soluble molecule in the colloidal range. BSA eluted during the constant field-strength portion of the fractionation with an estimated size of ca. 5 nm, close to a diameter of 7 nm based on the published value for the diffusion coefficient of BSA of  $5.9 \times 10^{-7} \text{ cm}^2 \text{ s}^{-1}$  (Sober 1970).

Prefiltered and preconcentrated Boothbay Harbor seawater sampled on two different days (17 April 1998 and 3 August 1998) revealed single broad particle peaks with peak height maxima eluting at 40 to 50 mL (Fig. 4). We calculated colloid size distributions using the standard curve equations relating bead diameter to retention volume, hypothesizing that

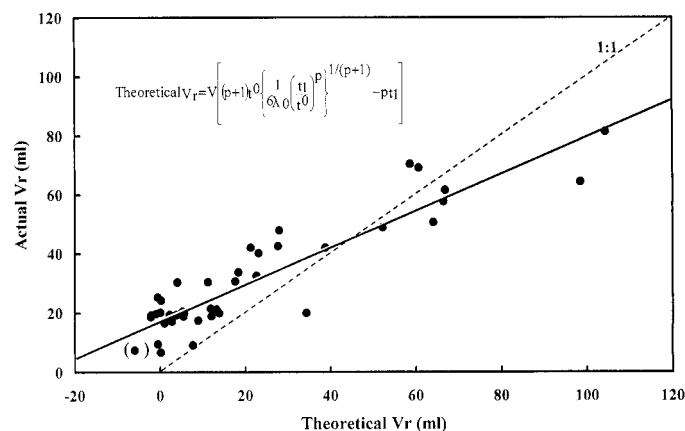


Fig. 3. Comparison of actual and theoretical (equation inset)  $V_r$  values for the 44 PS bead separations shown in Fig. 2. All bead separations were done under identical conditions except for variable channel flow rates, which are normalized by computing the  $V_r$  from the product of retention time  $t_r$  and  $V$ . The symbol in parentheses is the bovine serum albumin (BSA) sample and was excluded from the regression. The dashed line represents a slope of unity. The regression line intersects the 1:1 line at the approximate bead size of 500 nm.

the sum of the forces acting on the colloids causing them to separate in the channel was similar to that acting on the polystyrene bead standards. We acknowledge, however, that we have no a priori knowledge that the natural colloids exhibited the same anomalous retention behavior as the polystyrene beads. These results are shown in Table 1 and as the primary  $x$ -axes in Figs. 4 and 5. The colloid peaks extended from approximately 40 to 150 nm, with absorbance peak maxima centered at approximately 60 to 70 nm (Fig. 4).

The concentrated colloid sample from Fig. 4A, aged several days, was sized again to test the stability of the colloid size distributions (Fig. 5A). With time there appeared a second colloid peak that eluted at 80 to 90 mL, as well as the original peak at 40 to 50 mL. The second peak eluted outside the linear range of the standard curve in Fig. 2, but extrapolating out to this elution volume gives a mean colloid diameter value of approximately  $4 \mu\text{m}$  for the larger peak (Fig. 5A). A 5-min sonication did not significantly change the colloid size distribution (Fig. 5A, lower fractogram). A similar double-peak distribution was seen when the preconcentration step required 2 d to complete from Boothbay Harbor seawater sampled on 22 April 1998 (Fig. 5B). In addition to the second peaks being outside the linear range of the PS bead standards, it is also outside the range of the particle size range that is measurable by "normal mode" flow FFF, where particle retention is solely a function of particle diffusivity. While we know that a particle peak eluted at this volume and was likely the result of particle aggregation in the sample tube, we cannot assign any degree of confidence to the estimate of its mean diameter in Table 1 except to say that it was  $>1 \mu\text{m}$ . Transmission electron microscopy analyses of these FFF fractions dried on grids were inconclusive, as no colloids or larger aggregates were observed, most likely due to their low concentrations.

The underlying assumption in our flow FFF analyses was

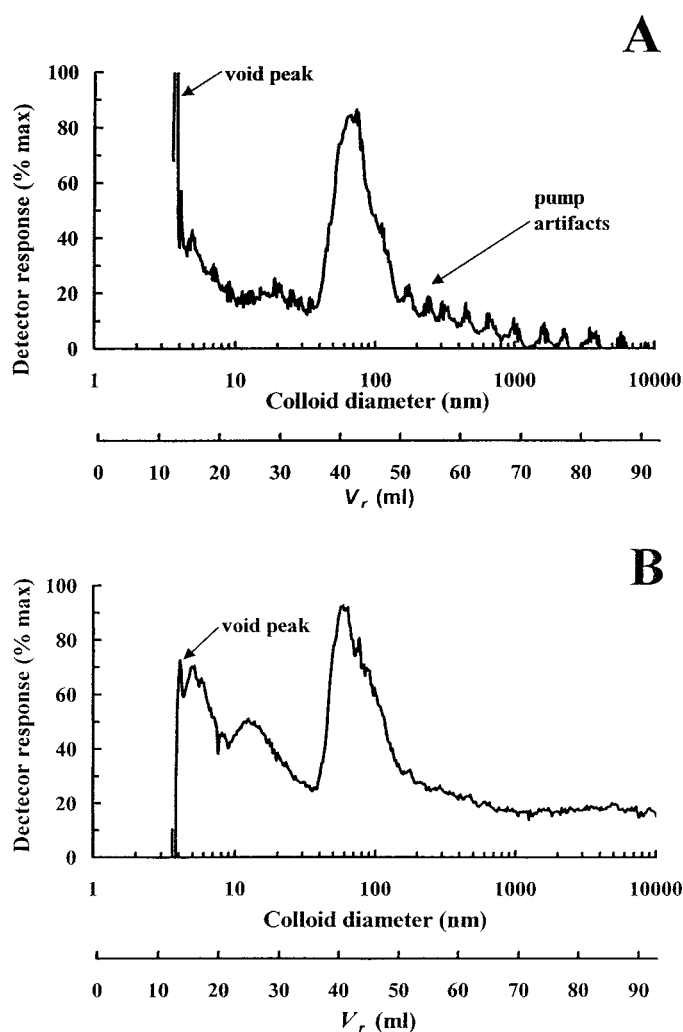


Fig. 4. Colloid size distribution of duplicate 1.0- $\mu\text{m}$ -filtered Boothbay Harbor seawater preconcentrated 2,200-fold in an Amicon concentrator with YM-10 membrane, followed by a subsequent concentration step in an MSI centrifuge concentrator. Fractogram A is for water sampled and concentrated on 17 April 1998, and B for water sampled and concentrated on 21 August 1998. Both samples were size fractionated immediately following the concentration step of the same day. Fractionation conditions for both separations were identical (detailed in text) except  $V = 3 \text{ ml min}^{-1}$  for B. Colloid size distributions were calculated from calibration lines in Fig. 2 where  $\log_{10}(\text{bead diameter}) = (V_r - 15)/27$ . Pump artifacts were due to worn channel pump seals and disappeared when they were replaced. The smaller peak in B between 10 and 20 nm was also apparent in a carrier solution blank. Ordinate axes scales are detector voltages expressed as a percent of maximum response.

that the predominant colloidal types present in our samples were roughly spherical in shape and displayed retention characteristics in the channel inherent to this shape and size, similar to the PS bead standards. Colloids isolated from surface waters of riverine, estuarine, and pelagic waters were shown by Santschi et al. (1998) to be fibrillar shaped with diameters of 1–3 nm and lengths of 100 to 2,000 nm. Colloids of quasispherical shape with diameters between 20 and 100 nm have been reported by Santschi et al. (1998) and by

Table 1. Colloid diameters and diffusion coefficients. Diameters were calculated from polystyrene bead standard curve (Fig. 2) and diffusion coefficients from the Stokes-Einstein equation,  $d_s = kT/3\pi\eta D$ , where  $d_s$  is the hydrodynamic diameter,  $k$  is Boltzmann's constant ( $1.38 \times 10^{-16} \text{ g cm}^2 \text{ s}^{-2} \text{ K}^{-1}$ ),  $T$  is the absolute temperature, and  $\eta$  is the viscosity of the carrier solution ( $0.011 \text{ g cm}^{-1} \text{ s}^{-1}$ ).

Sample	Mean ( $\pm$ sd) colloid diameter (nm)		Colloid diffusion coefficient ( $\times 10^{-8} \text{ g cm}^{-1} \text{ s}^{-1}$ )	
	Peak 1	Peak 2	Peak 1	Peak 2
Fig. 4A	68 (5)		6.5	
Fig. 4B	57 (4)		7.7	
Fig. 5A	60 (5)	>1	7.4	10.9
Fig. 5A (sonicated)	58 (5)	>1	7.6	10.9
Fig. 5B	60 (5)	>1	7.4	10.9

Wells and Goldberg (1991, 1994). Some fibrillar and quasi-spherical colloidal particles were aggregates of smaller and more numerous spheres and fibrils, with mixtures of both aggregates of spheres (Wells and Goldberg 1994) and spheres attached to fibrils (Santschi et al. 1998). Based on a rigorous mathematical treatment of the physical behavior of particles in the flow FFF channel, Giddings et al. (1976) estimated that the relationship between particle diffusivity and diameter is no longer predictable by the Stokes-Einstein equation (relating particle size to its diffusion coefficient) when the length-to-width ratio exceeds  $\sim 10$ , i.e., they cannot be accurately sized by flow FFF using spherical beads as standards. If the dominant colloidal particle present in our samples was fibrillar, then its diffusion properties would likely have retention characteristics different from that of a spherical bead standard. (We disregard the possibility for the moment that the colloid shapes and sizes reported by the above authors were artifacts of the TEM preparation process.) Similar errors related to shape would be expected for other sizing techniques, such as resistive-pulse particle counts, laser-light scattering (Theilking 1995), and flow cytometry (Phinney and Cucci 1989), all of which assume equivalent spherical diameters. In addition, ultrafiltration (Brownawell 1991), which assumes circular filter pores, and microscopic techniques (Wells and Goldberg 1994; Santschi et al. 1998), which dehydrate the sample, also potentially change particle sizes and shapes.

The UV detector response, comprising the ordinal data in the fractogram plots (expressed as percent maximum absorbance), is a complex function of particle size  $d$  and refractive index  $n$ , in accordance with Mie theory (Bricaud and Morel 1986). Using monodispersed suspensions of polystyrene beads of identical refractive index, we measured the detector's response while varying the size of the particle. These results are presented in Fig. 6, expressed as optical efficiency values as a function of particle diameter  $Q(d)$ , i.e., the proportion of the light incident on the particle's cross-sectional area that is either scattered or absorbed by the particle. Further, since we did not know the exact collection angle of the photodiode detector in our instrument, we do not know the amount of scattered light that is collected by the photodiode. We present modeled  $Q(d)$  values assuming both an infinitely shallow collection angle that omitted all the scattered radi-

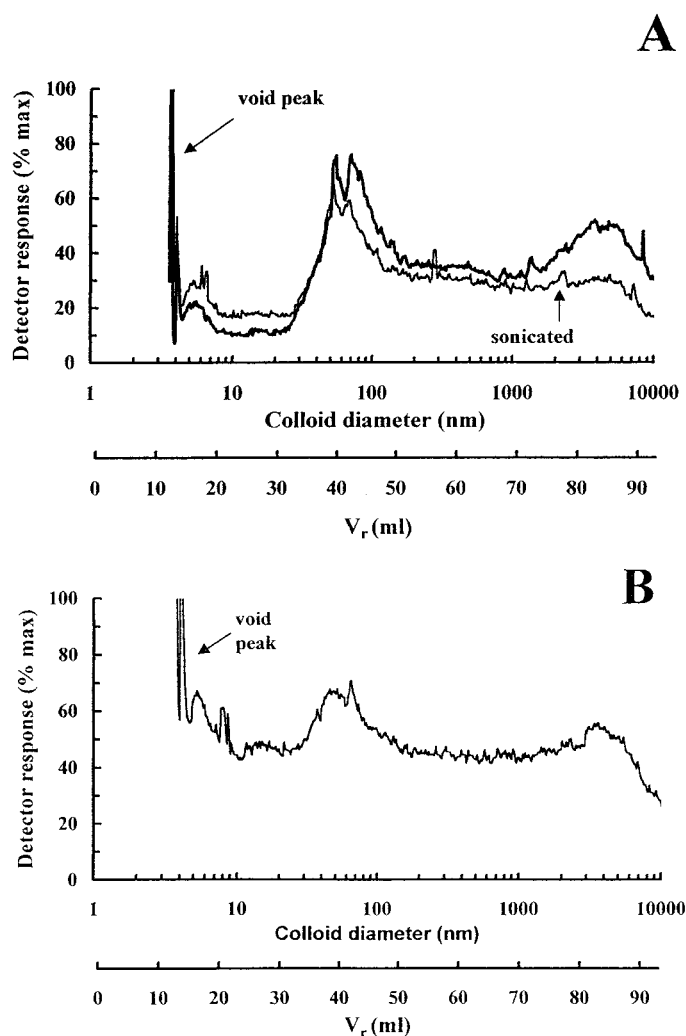


Fig. 5. Colloid size distribution of aged seawater concentrates. (A) The concentrated sample from 17 April (Fig. 4A) after sitting in dark at 4°C for 5 d (sampled 17 April and analyzed 22 April 1998). The lower fractogram in Fig. 4A is the same sample analyzed after 5 min of sonication to break up aggregates. Mean colloid diameters were not noticeably different after the sonication treatment. (B) The colloid size distribution of 1.0- $\mu\text{m}$ -filtered Boothbay Harbor seawater samples on 20 April 1998, preconcentrated 1,200-fold on top of a YM-10 membrane for 2 d and size fractionated at the end of the second day. All flow and channel conditions were the same as in Fig. 4A except the carrier solution was Sigma Sea salts (Sigma Chemical) reconstituted in MilliQ H<sub>2</sub>O to a final salinity of 25‰. The approximate diameters of the colloids composing the smaller and larger populations at their respective peak maxima were 60 and 4,000 nm, respectively. The colloid size distributions for all fractograms in this figure were calculated from the relationship in Fig. 2. Ordinate axes scales are detector voltages expressed as a percent of maximum response.

ations and thus measured attenuation (upper dark line), as well as assuming the detector collected all scattered radiations and thus acted as a true absorption meter (lower line). Since the size range of the PS beads spanned the regions where two different theoretical approaches apply, the Rayleigh and Van de Hulst's anomalous diffraction approxima-

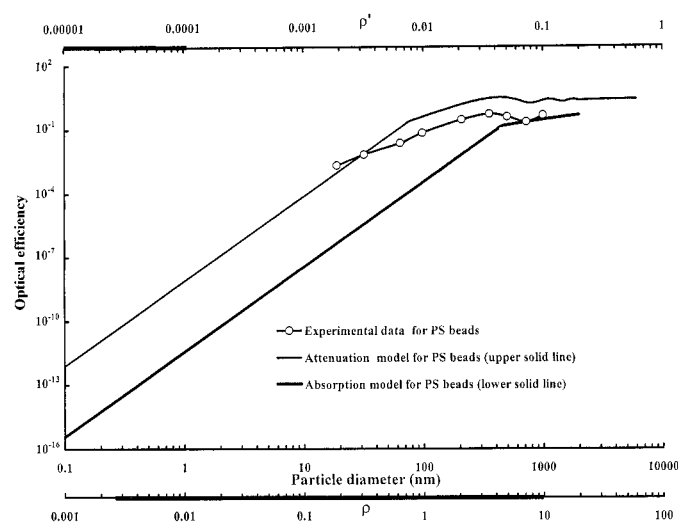


Fig. 6. Optical efficiency  $Q$  modeling of Alltech model 450 UV detector. Optical density at  $\lambda = 254$  nm (OD254) of monodispersed suspensions of polystyrene PS beads were measured and converted to an instrument optical efficiency parameter  $Q = (\text{OD}_{254} \times 2.303)/LCs$  (unitless), where  $L$  is the detector pathlength (0.007 m),  $C$  is the bead concentration (beads  $\text{m}^{-3}$ ; supplied by bead manufacturer and verified by flow cytometry),  $s$  is the bead cross-sectional area ( $\text{m}^2$ ), and 2.303 is to convert from base 10 to base  $e$  logarithm. Each symbol represents the mean of three replicate analyses. Error bars ( $\pm 1$  s.d.) are all smaller than the diameter of the symbols. The modeled scattering  $Qb$  and absorption  $Qa$  efficiencies for polystyrene were calculated as functions of  $\rho (= 2\pi d(n-1)/\lambda_w)$  and  $\rho' (= 4\pi d n' / \lambda_w)$ , respectively, where  $d$  is diameter,  $n$  and  $n'$  are the real and imaginary refractive indices at 254 nm relative to water, and  $\lambda_w$  is the wavelength in the medium. The  $n$  (1.33) and  $n'$  (0.0083) for PS at 254 nm were calculated using the Cauchy equation and data from Matheson and Saunderson (1952).  $Qb$  and  $Qa$  curves for PS were calculated using equations for the anomalous diffraction (Morel and Bricaud 1986) and Rayleigh (Van de Hulst 1957 table 8, p. 133) domains. The attenuation efficiency was the sum of the scattering and absorption efficiencies ( $Qc = Qb + Qa$ ). The attenuation and absorption Rayleigh and anomalous diffraction domain curves were connected where they intersected.  $Qc$  and  $Qa$  are shown for comparison to indicate the two possible extremes of optical geometries for the detector, as either an absorption (collecting all scattered radiations, i.e.,  $n'_s = 0.0083$  and  $n_s = n_{\text{medium}} = 1.38$ ) or as an attenuation meter (collected only the directly transmitted beam and excluded all scattered and absorbed radiations, i.e.,  $n'_s = 0.0083$  and  $n_s = 1.768$  [absorption coefficient and refractive index for polystyrene are calculated from the data of Matheson and Saunderson 1952]). The relationship  $Qc(\rho)$  corresponds to the upper solid line and uses the lower, second  $x$ -axis, and  $Qa(\rho')$  corresponds to the lower solid line and uses the upper, second  $x$ -axis. The solid bars on the  $x$ -axes denote tentative ranges of  $\rho$  and  $\rho'$  values for naturally occurring marine colloids (see text).

tion (Van de Hulst 1957), we used both models to treat the entire range of  $n$  and  $d$ . Two conclusions can be drawn from these data: (1) our experimental PS bead  $Q(d)$  values fell between the attenuation and the true absorption models, thus indicating that our detector measured an optical property intermediate between the two and is dependent upon the size and refractive index of the particle, and (2)  $Q(d)$  generally increased with increasing PS bead diameters until a maxi-

mum was reached. Thus, in our Alltech 450 UV detector, a 19-nm PS bead intercepted approximately 0.2% of the impinging 254-nm beam, while a 356-nm bead intercepted 57%.

We can constrain the variability in detector efficiency one may see when natural organic or mineralogic colloids are passed through our detector. Natural colloids vary over 3 orders of magnitude in diameter (1 to 1,000 nm), and we can estimate values of the real refractive index by using published values of  $n$  for marine phytoplankton's organic and inorganic material (proteins, carbohydrates, lipids, opal, and calcite) and recalculated for 254 nm using the Cauchy equation (Aas 1996) under the proviso that colloidal matter is derived from the physical or biological transformation of plankton-derived organic matter (Wells 1994). A tentative range of colloidal  $n'$  values can similarly be estimated using known values of absorption coefficients for the chemical constituents of marine plankton and the relationship  $n' = a_s \lambda / 4\pi$  (Morel and Bricaud 1986), where  $a_s$  is the absorption coefficient of the substance and  $\lambda$  is wavelength. Values estimated in this manner vary between 1.11 and 1.24 for  $n$ , and between 0 and  $1.1 \times 10^{-6}$  for  $n'$  at 254 nm, relative to seawater. The parameters  $n$  and  $d$  are incorporated in the parameter  $\rho (= 2\pi d[n - 1]/\lambda_w)$ , and  $n'$  and  $d$  in the parameter  $\rho' (= 4\pi d n'/\lambda_w)$ . The modeled lines in Fig. 6 for attenuation ( $Qc$ ) and absorption ( $Qa$ ) efficiencies can now be viewed as plotted versus  $\rho$  and  $\rho'$ , respectively (second and third  $x$ -axes), and incorporate all the variation  $Q$  due to natural variations in both  $n$  and  $d$  (for  $\rho$ ), and  $n'$  and  $d$  (for  $\rho'$ ). Colloidal  $Qc(\rho)$ , then, is shown to exhibit over 9 orders of magnitude variation ( $1 \times 10^{-10}$  to 3.3, black line on lower  $x$ -axis) across the estimated range of organic and inorganic colloid's physiochemical characteristics, or extremely low values of  $Qa$  (0 to  $4 \times 10^{-12}$ , black line on upper  $x$ -axis) depending on whether the UV detector was functioning as an absorption or attenuation meter. Thus our UV absorbance detector exhibited a large bias in sensitivity with smaller particles (<10 to 100 nm) largely undetected with respect to larger ones. We did not calculate variation due to nonsphericity of particles such as has been detected in TEM observations of colloid samples by Santschi et al. (1998; see below).

The preferred method of graphical representation of suspended particle size distribution is size-frequency distribution plots expressed either as particle number or volume distributions (Sheldon and Parsons 1967). The shape of such plots has been shown to be indicative of the nature and extent of biogeochemical transformations of organic matter in natural systems (Sheldon et al. 1972; McCave 1975). But without a priori knowledge of the refractive indices of the colloids at each size interval, it is not possible to transform our absorbance data into exact particle number distributions. However, since the range of possible  $n$  values for marine colloids is small compared to their size range (ca. twofold vs. 1,000-fold), it should be possible to estimate with minimal error the particle number distribution using some central or mean colloidal  $n$  value. Generally, this could be done by transforming our particle absorbance distribution data into particle number distributions using the relationship  $N/V = c/sQ_p$  (Bricaud and Morel 1986) where  $c$  is the atten-

uation coefficient at each size interval (derived from the detector OD254 output),  $s$  is the particle cross-sectional area,  $N/V$  is the particle number per unit volume of carrier, and  $Q_p$  is the  $n$ - and  $d$ -dependent optical efficiency. We are unable to perform this estimation with any fair degree of certainty, though, owing to the inability to distinguish the very low OD254 signal for the smaller diameter particles where the  $Q_p$  values are vanishingly small, from baseline noise. Erroneously attributing positive OD254 noise to particle attenuation would lead to exponentially large (ca.  $10^9$  or less) and incorrect  $N/V$  values. For this reason, examining particle size distributions using microscopy (Harris 1977; Wells and Goldberg 1991, 1994; Santschi et al. 1998) and particle-resistance counters (Koike et al. 1990; Longhurst et al. 1992; Chin et al. 1998) are more quantitative than flow FFF methods as they measure the absolute number of particles directly, albeit with the potential problems associated with dehydration during sample preparation mentioned above.

Future work using flow FFF to size-fractionate colloids should explore the use of other standards that mimic as closely as possible the known conformations and chemical behaviors of colloids observed in aquatic systems. A similar problem sizing humic substances was overcome by Beckett et al. (1987) by using commercially available reference humate samples of known molecular weight to determine molecular weight calibration coefficients. No such reference colloid sample exists at this time for marine colloids (Brownawell 1991), and it is likely that no one reference colloid can be found to mimic closely the great variety of shapes, sizes, and surface chemical properties of colloids found in nature. Some size standard candidates for flow FFF analysis, though, would be water-soluble, anionic polymers such as polystyrenesulfonate (Benincasa and Giddings 1992), colloidal silicas (Giddings et al. 1978), pure and concentrated suspensions of marine viruses whose sizes have been verified with TEM (Giddings et al. 1977), and globular and linear protein, polysaccharide, or plasmid size standards (Wahlund and Litzén 1989). The protein and polysaccharide size standards mentioned last may come closest to a true reference colloid given the preponderance of these materials reported in the colloidal size fraction in some marine systems (Maurer 1976; Benner et al. 1992).

With careful attention paid to experimental conditions to avoid potential experimental artifacts and prudent selection of particle size standards to characterize the channel dimensions, flow FFF is a viable technique for sizing a wide range of submicron particles in natural waters. Its main advantages are that the particles are analyzed in their native physiochemical environment of seawater, thus avoiding potential conformational and size changes associated with changes in pH and ionic strength (Chin et al. 1998). When power-programmed field decay is used to vary the field strength, a wide range of particle sizes spanning the entire colloidal size range can be separated in a single run with equal resolving power attained throughout the range. Also, with minimal modification of the separation conditions, one can use flow FFF in steric separation mode to separate larger particles  $>1 \mu\text{m}$ , thus extending the particle size range of the analysis from approximately 5 nm to  $50 \mu\text{m}$  or greater (Giddings et al. 1987). The use of a more sensitive detector (and cleaner

natural seawater carrier solutions) to lower the detection limit for colloids could possibly eliminate the need for preconcentration of sample with its potential artifacts of aggregation. We emphasize the limitation of using a scattering or absorption detector as the means of quantifying eluting particle mass, due to the extremely small optical efficiencies in this size and refractive index region. Future work will concentrate on using flow-through detectors that count the passage of individual particles as they elute from the FFF channel. One possibility that holds promise is to collect discrete, small volume fractions, stain the particles with chemical-specific fluorescent stains, and measure the number concentrations on a flow cytometer. Other possible pitfalls in using flow FFF to analyze submicron particulates are sample overloading and nonequilibrium zone broadening, which are more completely outlined by Giddings and Caldwell (1984).

*Robert D. Vaillancourt and William M. Balch*

Bigelow Laboratory for Ocean Sciences  
McKown Point Road  
West Boothbay Harbor, Maine 04575

## References

- AAS, E. 1996. Refractive index of phytoplankton derived from its metabolite composition. *J. Plankton Res.* **18**: 2223–2249.
- BECKETT, R., Z. JUE, AND J. C. GIDDINGS. 1987. Determination of molecular weight distributions of fulvic and humic acids using flow field-flow fractionation. *Environ. Sci. Technol.* **21**: 289–295.
- BENINCASA, M. A., AND J. C. GIDDINGS. 1992. Separation and molecular weight distribution of anionic and cationic water-soluble polymers by flow field-flow fractionation. *Anal. Chem.* **64**: 790–798.
- BENNER, R., J. D. PAKULSKI, M. MCCARTHY, J. I. HEDGES, AND P. G. HATCHER. 1992. Bulk chemical characteristics of dissolved organic matter in the ocean. *Science* **255**: 1561–1564.
- BRICAUD, A., AND A. MOREL. 1986. Light attenuation and scattering by phytoplanktonic cells: A theoretical modeling. *Appl. Opt.* **25**: 571–580.
- BROWNAWELL, B. J. 1991. Methods for isolating colloidal organic matter from seawater: General considerations and recommendations. *In* Marine particles: Analysis and characterization. Geophysical Monograph 63. Am. Geophys. Union.
- BUFFLE, J., P. DELADOEY, AND W. HAERDI. 1978. The use of ultrafiltration for the separation and fractionation of organic ligands in fresh waters. *Anal. Chim. Acta* **101**: 339–357.
- CHIN, W. C., M. V. ORELLANA, AND P. VERDUGO. 1998. Spontaneous assembly of marine dissolved organic matter into polymer gels. *Nature* **391**: 568–572.
- GIDDINGS, J. C., AND K. D. CALDWELL. 1984. Field-flow fractionation: Choices in programmed and nonprogrammed operation. *Anal. Chem.* **56**: 2093–2099.
- , X. CHEN, K. G. WAHLUND, AND M. N. MYERS. 1987. Fast particle separation by flow/steric field-flow fractionation. *Anal. Chem.* **59**: 1957–1962.
- , G. C. LIN, AND M. N. MYERS. 1978. Fractionation and size analysis of colloidal silica by flow field-flow fractionation. *J. Coll. Int. Sci.* **65**: 67–78.
- , M. N. MYERS, F. J. YANG, AND L. K. SMITH. 1976. Mass analysis of particles and macromolecules by field-flow fractionation. p. 381–398. *In* M. Kerker [ed.], *Colloid and interface science*. Academic.
- , F. J. YANG, AND M. N. MYERS. 1977. Flow field-flow fractionation: New method for separating, purifying, and characterizing the diffusivity of viruses. *J. Virol.* **21**: 131–138.
- HARRIS, J. E. 1977. Characterization of suspended matter in the Gulf of Mexico—II Particle size analysis of suspended matter from deep water. *Deep-Sea Res.* **24**: 1055–1061.
- HONEYMAN, B. D., AND P. H. SANTSCHI. 1991. Coupling adsorption and particle aggregation: Laboratory studies of “colloidal pumping” using <sup>59</sup>Fe-labeled hematite. *Environ. Sci. Technol.* **25**: 1739–1747.
- KEPKAY, P. E. 1994. Particle aggregation and the biological reactivity of colloids. *Mar. Ecol. Prog. Ser.* **109**: 293–304.
- KOIKE, I., S. HARA, K. TERAUCHI, AND K. KOGURE. 1990. Role of sub-micrometer particles in the ocean. *Nature* **345**: 242–244.
- LOEB, G. I., AND R. A. NIEHOF. 1977. Adsorption of an organic film at the platinum-seawater interface. *J. Mar. Res.* **35**: 283–291.
- LONGHURST, A. R., AND OTHERS. 1992. Sub-micron particles in northwest Atlantic shelf water. *Deep-Sea Res.* **39**: 1–7.
- MATHESON, L. A., AND J. L. SAUNDERSON. 1952. Optical and electrical properties of polystyrene, p. 517–573. *In* R. H. Bundy and R. F. Boyer [eds.], *Styrene, its polymers, copolymers and derivatives*. Am. Chem. Soc. Monogr. Ser.
- MAURER, L. G. 1976. Organic polymers in seawater: Changes with depth in the Gulf of Mexico. *Deep-Sea Res.* **23**: 1059–1064.
- MCCAVE, I. N. 1975. Vertical flux of particles in the ocean. *Deep-Sea Res.* **22**: 491–502.
- MOREL, A., AND A. BRICAUD. 1986. Inherent optical properties of algal cells including picoplankton: Theoretical and experimental results. *Can. Bull. Fish. Aquat. Sci.* **214**: 521–559.
- NEIHOF, R. A., AND G. I. LOEB. 1972. The surface charge of particulate matter in seawater. *Limnol. Oceanogr.* **17**: 7–16.
- PHINNEY, D. A., AND T. CUCCI. 1989. Flow cytometry and phytoplankton. *Cytometry* **10**: 511–521.
- SANTSCHI, P. H., E. BALNOIS, K. J. WILKINSON, J. ZHANG, AND J. BUFFLE. 1998. Fibrillar polysaccharides in marine macromolecular organic matter as imaged by atomic force microscopy and transmission electron microscopy. *Limnol. Oceanogr.* **43**: 896–908.
- SHELDON, R. W., AND T. R. PARSONS. 1967. A continuous size spectrum for particulate matter in the sea. *J. Fish. Res. Board Can.* **24**: 909–915.
- , A. PRAKASH, AND W. H. SUTCLIFFE, JR. 1972. The size distribution of particles in the ocean. *Limnol. Oceanogr.* **27**: 327–340.
- SOBER, H. A. 1970. *Handbook of Biochemistry*, 2nd ed. Chemical Rubber. Section C.
- STRAMSKI, D., AND D. A. KIEFER. 1991. Light scattering by microorganisms in the open ocean. *Prog. Oceanogr.* **28**: 343–383.
- THEILKING, H., D. ROESSNER, AND W. M. KULICKE. 1995. On-line coupling of flow field-flow fractionation and multiangle laser light scattering for the characterization of polystyrene beads. *Anal. Chem.* **67**: 3229–3233.

## Acknowledgements

We are indebted to Paty Matrai for the loan of her Amicon concentrators, Brian Yocis for instructions on their use, and Terry Cucci for bead standards and flow cytometric analysis. Technical advice provided by Marcia Hansen, Mike Miller, and Andreas Kummerow at FFFractionation is greatly appreciated. We also thank two anonymous reviewers for their helpful comments. This study was supported by ONR (N00014-91J-1048), NASA (NAGW 2426; NAS5-31363), and NSF (OCE-9596167). This is Bigelow Laboratory for Ocean Sciences contribution number 99005.

- VAN DE HULST, H. C. 1957. Light scattering by small particles. Dover.
- VOLD, R. D., AND M. J. VOLD. 1966. Colloid chemistry, p. 263–265. *In* Encyclopedia of Chemistry. Reinhold.
- WAHLUND, K. G., AND A. LITZÉN. 1989. Application of an asymmetrical flow field-flow fractionation channel to the separation and characterization of proteins, plasmids, plasmid fragments, polysaccharides and unicellular algae. *J. Chromatogr.* **461**: 73–87.
- WELLS, M. L., AND E. D. GOLDBERG. 1991. Occurrence of small colloids in sea water. *Nature* **353**: 342–344.
- , AND ———. 1994. The distribution of colloids in the North Atlantic and Southern Oceans. *Limnol. Oceanogr.* **39**: 286–302.
- WILLIAMS, P. S., AND J. C. GIDDINGS. 1987. Power programmed field-flow fractionation: A new program form for improved uniformity of fractionating power. *Anal. Chem.* **59**: 2038–2044.
- ZSOLNAY, A. 1979. Coastal colloidal carbon: A study of its seasonal variation and the possibility of river input. *Estuar. Coast. Mar. Sci.* **9**: 559–567.

Received: 10 February 1999  
Accepted: 13 October 1999  
Amended: 31 October 1999

*Limnol. Oceanogr.*, 45(2), 2000, 492–498  
© 2000, by the American Society of Limnology and Oceanography, Inc.

## Light scattering by viral suspensions

**Abstract**—Viruses represent one of the most abundant, ocean-borne particle types and have significant potential for affecting optical backscattering. Experiments addressing the light-scattering properties of viruses have heretofore not been conducted. Here we report the results of laboratory experiments in which the volume-scattering functions of several bacterial viruses (bacteriophages) were measured at varying concentrations with a laser light-scattering photometer using a He-Ne and/or Argon ion laser (632.8 and 514.0 nm, respectively). Four bacterial viruses of varying size were examined, including the coliphages MS-2 (capsid size 25–30 nm) and T-4 (capsid size ~100 nm), and marine phages isolated from Saco Bay, Maine (designation Y-1, capsid size 50–80 nm) and Boothbay Harbor, Maine (designation C-2, capsid size ~110 nm). Volume-scattering functions (VSFs) were fitted with the Beardsley-Zaneveld function and then integrated in the backward direction to calculate backscattering cross section. This was compared to the virus geometric cross section as determined by transmission electron microscopy and flow-field fractionation. Typical backscattering efficiencies varied from  $20 \times 10^{-6}$  to  $1,000 \times 10^{-6}$ . Data on particle size and backscattering efficiencies were incorporated into Mie scattering calculations to estimate refractive index of viruses. The median relative refractive index of the four viruses was ~1.06. Results presented here suggest that viruses, while highly abundant in the sea, are not a major source of backscattering.

Radiative transfer in the ocean is driven by the optical properties of seawater, its suspended particles, and dissolved compounds. While the optical properties of pure sea water and particles  $>1 \mu\text{m}$  are reasonably well understood (Morel and Ahn 1991; Mobley 1994), the inherent optical properties (absorption and scattering) of submicron particles and dissolved matter are less well known, particularly in the micrometer to nanometer range. This size range includes the smallest algae, most bacteria, viruses, and colloids. In ocean optics, researchers have used a reductionistic approach to describe the inherent optical properties of the individual components. For example, phytoplankton are given one set

of specific absorption and scattering coefficients, while bacteria, which scatter more than they absorb, are given a different set of coefficients. This reductionistic approach to closure has revealed a large discrepancy between observed and predicted inherent optical properties, namely, when the optically scattering fractions are summed and compared to measured light scattering, only 50–75% of the total scattering can be accounted for by particles  $>0.5 \mu\text{m}$  (i.e., closure is not attained).

Experimental closure becomes even less attainable when one considers backscattered light, that is, the volume scattering integrated over all backward directions. Backscattering and absorption are important because they are used for predicting remote-sensing reflectance. Previous studies have shown that optical backscattering ( $b_b$ ) by the various particle types described above (all  $>0.5 \mu\text{m}$ ) represents an insignificant fraction of the total backscattering coefficient, accounting for ~10% of the total  $b_b$  (Morel and Ahn 1991; Stramski and Kiefer 1991). Models have suggested that 3- $\mu\text{m}$  particles are responsible for most of the total light scattering in the ocean, with particles  $\leq 0.1 \mu\text{m}$  responsible for the bulk of the backscattering coefficient (Morel and Ahn 1991; but note that Stramski and Kiefer [1991] were less restrictive and suggested that most backscattering came from particles  $<1 \mu\text{m}$ ). Particles smaller than  $0.1 \mu\text{m}$  would be considered dissolved given the operational definition of dissolved organic matter (i.e., anything passing through a 0.2- $\mu\text{m}$  filter). The composition of these particles is unknown, but may include colloidal particles smaller than  $0.6 \mu\text{m}$ , such as Koike particles (Koike et al. 1990), microgels (Chin et al. 1998), or viruses.

Viruses represent an abundant, diverse, and important component of the suspended matter in the world ocean (Boersheim et al. 1990; Hara et al. 1991), with concentrations ranging from  $10^6$  to as high as  $10^{14} \text{ m}^{-3}$  in eutrophic regions (Bergh et al. 1989; Kepner et al. 1998). Viruses infect all members of the marine plankton and are thought to play an important role in the ecological control of planktonic microorganisms (Proctor and Fuhrman 1990;